Supporting Information

Porous Interdigitation Molecular Cage from Tetraphenylethylene Trimeric Macrocycles that Showed Highly Selective Adsorption of CO_2 and TNT Vapor in Air

Jia-Bin Xiong,[†] Jin-Hua Wang,[†] Bao Li,[†,*] Chun Zhang,[‡,*] Bien Tan,[†,*] and Yan-Song Zheng,[†,*]

[†]School of Chemistry and Chemical Engineering, Huazhong University of Science and Technology, Wuhan 430074, China. zyansong@hotmail.com.
[‡]College of Life Science and Technology, Huazhong University of Science and Technology.
Address: Wuhan 430074, China

Table of Contents

Materials and Method…………………………………………………………………	2
Detection of TNT vapor………………………………………………………….............	2
Synthesis of the TPE macrocycle **5**…………………………………………………	3
Fig. S1−Fig. S12, Characteristic spectra of compounds **2**, **3** and **5**……………………	5−14
Fig. S13. The absorption spectra of **5**…………………………………………………….	15
Fig. S14. Change in fluorescence spectra of **5** with water fraction……………………	15
Fig. S15. The cage from **5** shown in spacefill style…………………………………..	16
Fig. S16. XRD pattern of **5** and Analog structure…………………………………….	16
Fig. S17. Initial gas uptake slopes of cage **5** at 273K…………………………………	17
Fig. S18. Isosteric heat of adsorption for CO_2 at different CO_2 loadings……………	17
Fig. S19. Fluorescence change of **5** in 95:5 H_2O/THF with TNT……………………	18
Fig. S20. Fluorescence change of **5** in the presence of 1% $NaNO_3$ with TNT……….	18
Fig. S21. The fluorescence intensity ratio ($I_0/I – 1$) of **5** with concentration of TNT…	19
Fig. S22. Linear fitting for change of ($I_0/I – 1$) of **5** with TNT…………………….....	19−20
Fig. S23. Fluorescence change of **5** in 95:5 H_2O/THF without salt with TNT vapor…	20
Fig. S24. Change of I/I_0 ratios of **5** in the presence of 1% salts with TNT vapor…….	21
Fig. S25. Change of I/I_0 ratios of **5** with volume ratio of TNT Vapor………………...	21
Fig. 26. Linear fitting of I/I_0 ratios of **5** with volume ratio of TNT-saturating air…….	22

Materials and method

Materials: All reagents and solvents were chemical pure (CP) grade or analytical reagent (AR) grade and were used as received unless otherwise indicated.

Measurements: ^{1}H NMR and ^{13}C NMR spectra were measured on a Bruker AV 400 spectrometer at 298 K in $CDCl_3$. Infrared spectra were recorded on BRUKER EQUINAX55 spectrometer. Absorption spectra were recorded on a Hewlett Packard 8453 UV–Vis spectrophotometer. Mass spectrum was measured on an Ion Spec 4.7 Tesla FTMS instrument. Fluorescent emission spectra were collected on a Shimadzu RF-5301 fluorophotometer at 298 K.

Growth and measurements of single crystals: The single crystal of **5** or TNT-**5** complex was obtained by standing the hot solution of **5** or mixture of TNT and **5** (molar ratio 5:1) in DMSO at 30 ^{o}C for about one week. X-ray diffraction data of **5** and **TNT-5** were collected via Rigaku XtaLAB P200 using Mo-$K\alpha$ (λ = 0.71073 Å) radiation. The structures of complexes were solved by direct methods, and the non-hydrogen atoms were located from the trial structure and then refined anisotropically with SHELXTL-16 using a full-matrix least squares procedure based on F^2 values. The *PLATON/SQUEEZE* routine was employed to calculate the diffraction contribution from the solvent molecules, and thereby to produce a set of solvent-free diffraction intensities for **5**.

Preparation of solvent-treated crystals of TNT-5 complex: Crystals of TNT-**5** complex precipitated from DMSO were immersed in methanol for 4 h and then filtered. The collected solid was again immersed in methanol for 4 h and filtered. This process was repeated for four times. Finally, the obtained solid was treated with ethyl ether just like methanol to give solvent-treated crystals as a powder.

Gas Sorption Analysis. Surface areas and pore size distributions were measured by nitrogen adsorption and desorption at 77 K using a Micromeritics ASAP 2020 volumetric adsorption analyzer. Sample was degassed at 120 °C for 10 h under vacuum before analysis. N_2 isotherms were measured at 273 K up to 1.0 bar using a Micromeritics ASAP 2020 volumetric adsorption analyzer with the same degassing procedure. CO_2 isotherms were measured at 273 and 298 K up to 1.0 bar using a Micromeritics ASAP 2020 volumetric adsorption analyzer with the same degassing procedure.

Computational Details. The surface areas were calculated from nitrogen adsorption data by Brunauer-Emmett-Teller (BET) adsorption models. Pore size distributions were calculated by DFT methods via the adsorption branch.

Detection of TNT vapor in air

Preparation of TNT-saturating air: About 100 mg of TNT were added in a 5 L of bottle and let TNT fully evaporate into the air in the bottle by standing it at 25 °C for 24 h.

Preparation of TNT vapor diluted by air: Into the bottom of a 5 L of bottle was injected 500 mL of TNT-saturating air by syringe. Upon lidded, the bottle was standing for 1 h to give TNT-vapor diluted 10 times. Other TNT-vapor samples with different dilution times were prepared in the same way.

The suspension preparation of 5 in H_2O/THF 95:5: Solution of the macrocycle **5** in THF was rapidly injected into water without or with $NaNO_3$ by syringe. The mixture was shaken once the injection was finished to give the suspension.

The TNT-containing air was slowly bubbled into the suspension of the macrocycle **5** by a 20 mL of syringe. The bubbling speed is about 3-5 bubbles per second. As soon as the addition was ended, the suspension was measured for its fluorescence intensity.

Synthesis of the TPE macrocycle 5:

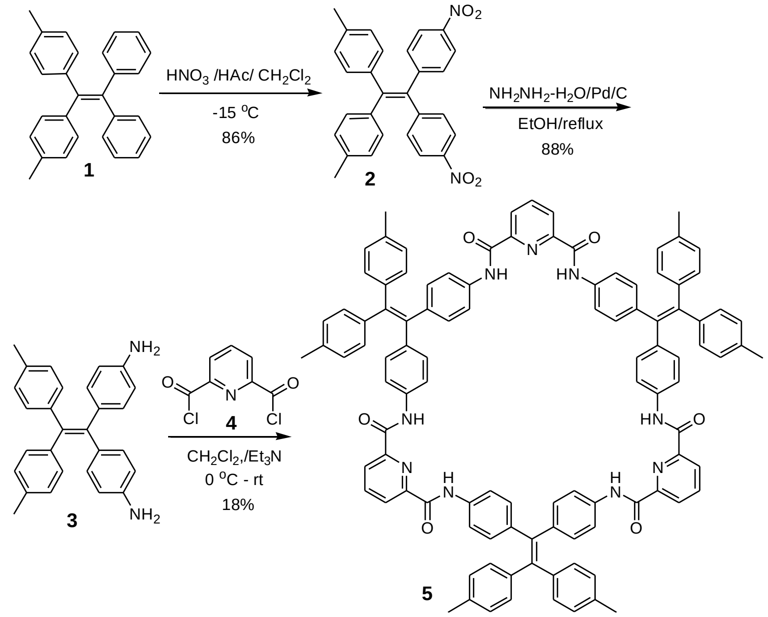

Synthesis of compound 2. To a 250 mL round bottom flask were added **1** (14.4 g, 40 mmol), acetic acid (11.5 mL, 200 mmol) and dichloromethane (160 mL). The resultant mixture was cooled to –15 ^{o}C under stirring before concentrated nitric acid (1.6 mL, 24 mmol) was added. The reaction mixture was continued to stir at this temperature for 30 min before it was poured into ice water. The organic layer was separated and washed with water three times. Upon drying over anhydrous sodium sulfate and filtration, the solution was evaporated to dryness. The residue was recrystallized with dichloromethane and methanol to give **2** as yellow solid (15.4 g, 86%): mp 174–175 ^{o}C; ^{1}H NMR (400 MHz, $CDCl_3$) δ 7.99 (d, J = 8.6 Hz, 4H), 7.15 (d, J = 8.6 Hz, 4H), 6.95 (d, J = 8.0 Hz, 4H), 6.87 (d, J = 8.0 Hz, 4H), 2.28 (s, 6H) ppm; ^{13}C NMR (100 MHz, $CDCl_3$) δ 150.0, 146.9, 146.2, 138.9, 138.0, 135.5, 132.0, 131.1, 128.9, 123.3, 21.2 ppm; IR (KBr) v_{max} 3072, 2920, 1592, 1514, 1339, 1108, 818, 753, 483, cm^{-1}; HRMS (ESI-TOF) m/z $[M]^+$ calcd for $C_{28}H_{22}N_2O_4$ 450.1580, found 450.1589.

Synthesis of compound 3. To a 250 mL round bottom flask were added **2** (3.0 g, 6.7 mmol), Pd/C (10%, 160 mg, 0.15 mmol) and dried ethanol (120 mL). The resultant mixture was stirred at room temperature for 10 minutes before hydrazine hydrate (85%, 19.4 mL, 340 mmol) was added. After refluxing for 4 hours, the reaction mixture was cooled to room temperature and filtered through a layer of Celite. The filtrate was evaporated to dryness and the obtained solid was dissolved in dichloromethane (60 mL). After the solution was washed with water for three times, dried over anhydrous sodium, and filtered, the solvent was removed under reduced pressure. The residue was recrystallized with dichloromethane and methanol to afford **3** as slightly yellow solid (2.3 g 88%): mp 243–244 ^{o}C; ^{1}H NMR (400 MHz, $CDCl_3$) δ 6.91 (d, J = 8.8 Hz, 4H), 6.88 (d, J = 8.8 Hz, 4H), 6.80 (d, J = 8.4 Hz, 4H), 6.40 (d, J = 8.4 Hz, 4H), 2.24 (s, 6H) ppm; ^{13}C NMR (100 MHz, $CDCl_3$) δ 144.4, 142.0, 139.9, 137.6, 135.2, 135.0, 132.5, 131.3, 128.3, 114.3, 21.2 ppm; IR (KBr) v_{max} 3429, 3350, 3022, 1621, 1511, 1271, 1176, 822, 771, 737, 578, 470, cm^{-1}; HRMS (ESI-TOF) m/z $[M]^+$ calcd for $C_{28}H_{26}N_2$ 390.2096, found 390.2078.

Synthesis of compound 5. To a round bottom flask were added 2,6-pyridinedicarboxyl chloride **4** (0.53 g, 2.6 mmol), compound **3** (1.0 g, 2.6 mmol), Et_3N (2.1 mL, 15.6 mmol) and dried dichloromethane (150 mL). After the reaction mixture was stirred overnight, it was washed three times with water. The organic layer was dried over anhydrous sodium sulfate, filtered, and evaporated under vacuum. The residue was purified by flash chromatography (silica gel; eluent dichloromethane / methanol 85 / 1) to give **5** as light yellow solid (240 mg, 18%): mp >300 ^{o}C; ^{1}H NMR (400 MHz, $CDCl_3$) δ 9.43 (s, 6H), 8.46 (d, *J* = 7.8 Hz, 6H), 8.14 (t, *J* = 7.8 Hz, 3H), 7.50 (d, *J* = 8.5 Hz, 12H), 7.05 (d, *J* = 4.2 Hz, 12H), 6.91 (s, 24H), 2.24 (s, 6H); ^{13}C NMR (100 MHz, $CDCl_3$) δ 160.6, 148.8, 141.5, 140.9, 140.5, 139.9, 138.1, 136.3, 135.1, 132.1, 131.1, 128.5, 125.5, 119.1, 21.2; IR (KBr) *v* 3389, 3319, 3027, 2922, 1686, 1582, 1520, 1405, 864, 819 cm^{-1}; HRMS (ESI-TOF) m/z calcd for $C_{106}H_{82}N_9O_6$ [M+H] 1564.6388, found 1564.6299 [M+H].

Characteristic spectra of compounds 2, 3 and 5.

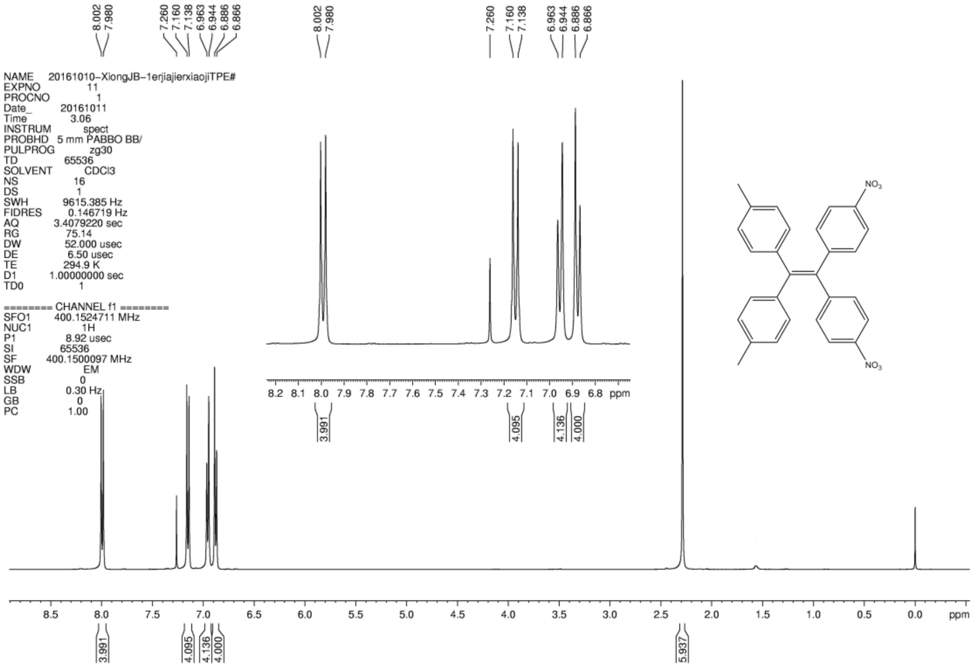

Fig. S1. ^{1}H NMR spectrum of compound **2**.

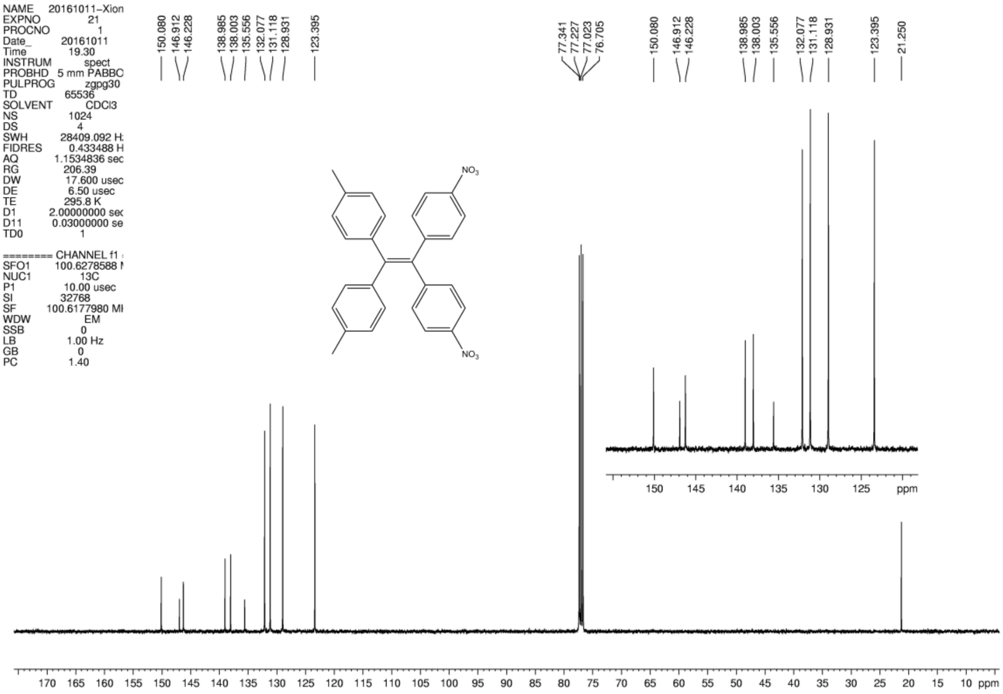

Fig. S2. ^{13}C NMR spectrum of compound **2**.

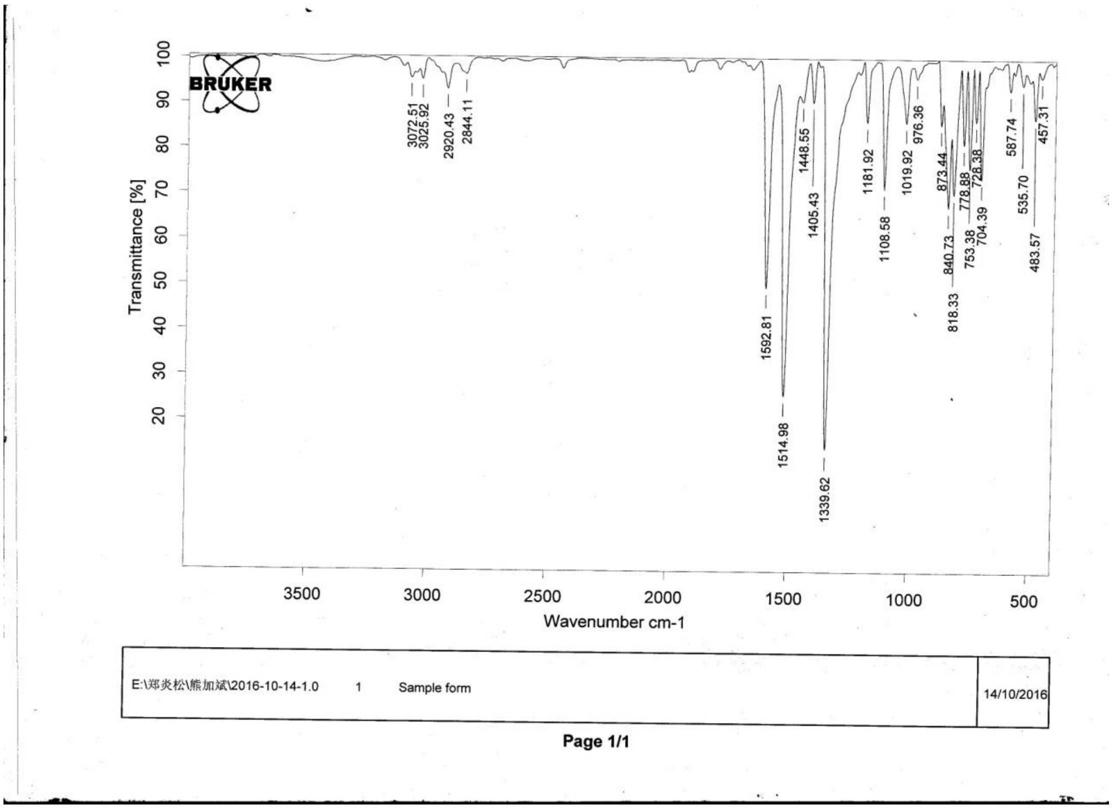

Fig. S3. IR spectrum of compound **2**.

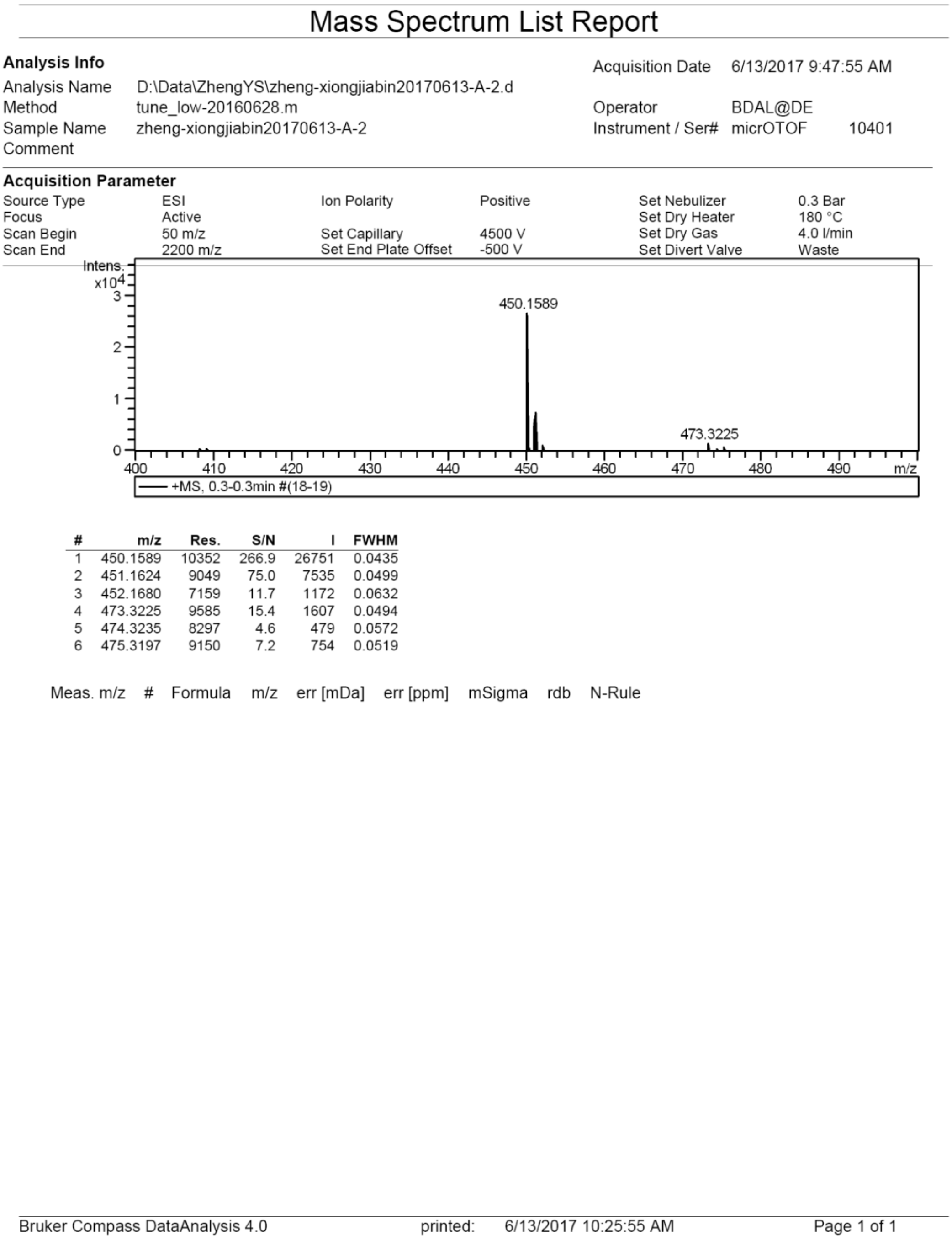

Mass Spectrum List Report

Analysis Info

Analysis Name	D:\Data\ZhengYS\zheng-xiongjiabin20170613-A-2.d	Acquisition Date	6/13/2017 9:47:55 AM
Method	tune_low-20160628.m	Operator	BDAL@DE
Sample Name	zheng-xiongjiabin20170613-A-2	Instrument / Ser#	micrOTOF 10401
Comment			

Acquisition Parameter

Source Type	ESI	Ion Polarity	Positive	Set Nebulizer	0.3 Bar
Focus	Active			Set Dry Heater	180 °C
Scan Begin	50 m/z	Set Capillary	4500 V	Set Dry Gas	4.0 l/min
Scan End	2200 m/z	Set End Plate Offset	-500 V	Set Divert Valve	Waste

#	m/z	Res.	S/N	I	FWHM
1	450.1589	10352	266.9	26751	0.0435
2	451.1624	9049	75.0	7535	0.0499
3	452.1680	7159	11.7	1172	0.0632
4	473.3225	9585	15.4	1607	0.0494
5	474.3235	8297	4.6	479	0.0572
6	475.3197	9150	7.2	754	0.0519

Meas. m/z	#	Formula	m/z	err [mDa]	err [ppm]	mSigma	rdb	N-Rule

Bruker Compass DataAnalysis 4.0 printed: 6/13/2017 10:25:55 AM Page 1 of 1

Fig. S4. HRMS spectrum of compound **2**.

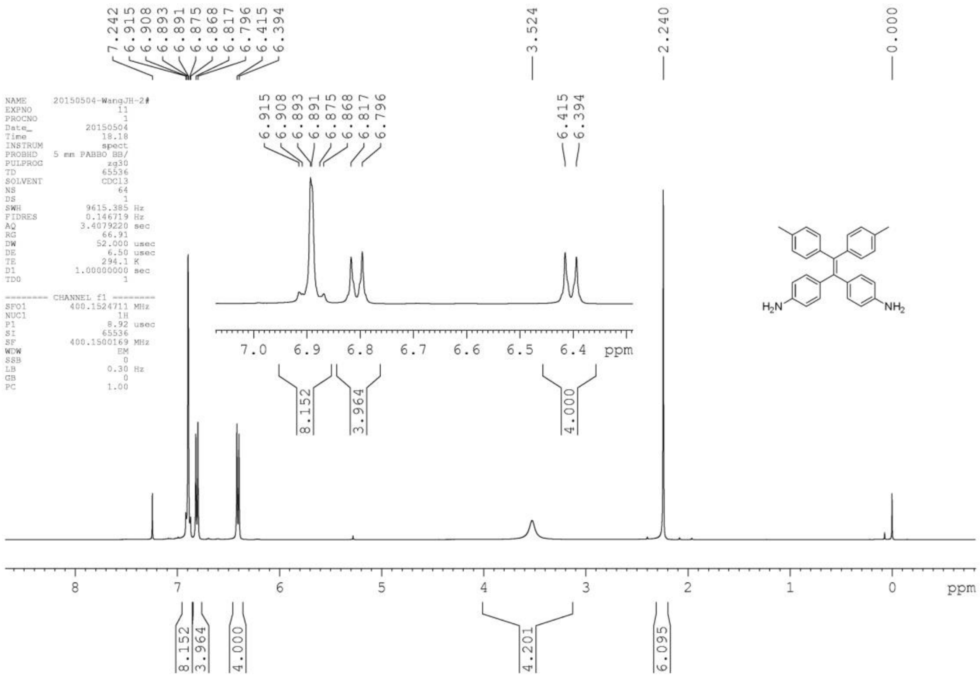

Fig. S5. ^1H NMR spectrum of compound **3**.

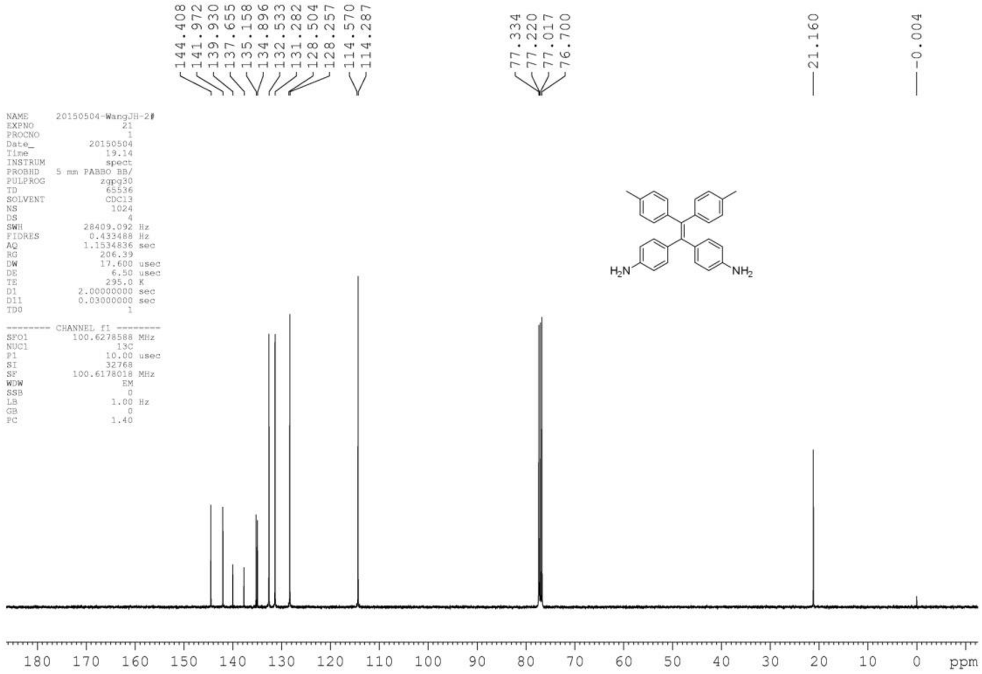

Fig. S6. ^{13}C NMR spectrum of compound **3**.

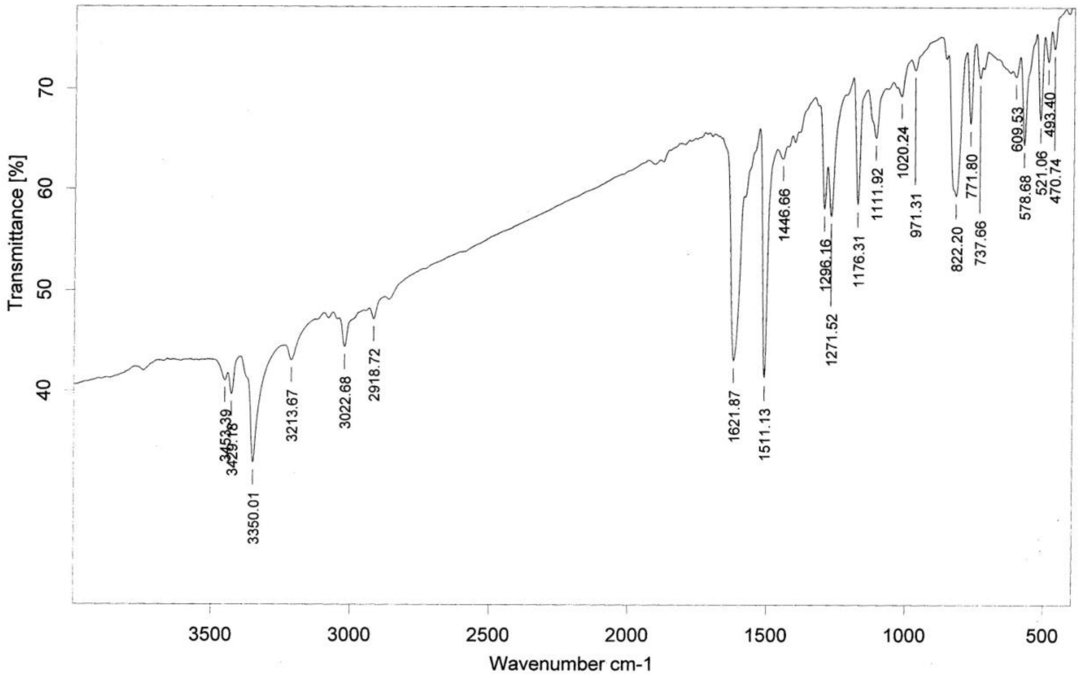

Fig. S7. IR spectrum of compound **3**.

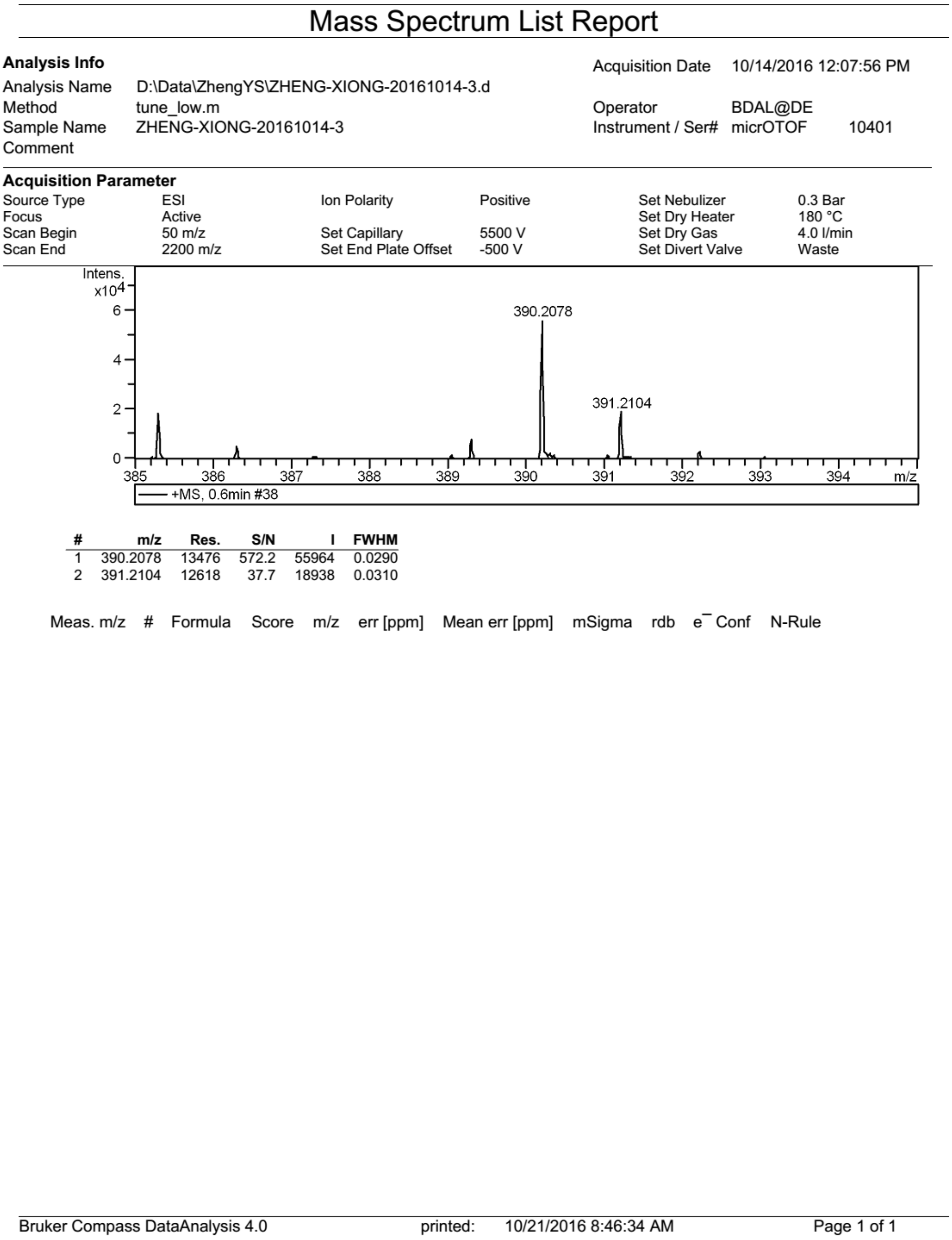

Mass Spectrum List Report

Analysis Info

Analysis Name	D:\Data\ZhengYS\ZHENG-XIONG-20161014-3.d	Acquisition Date	10/14/2016 12:07:56 PM
Method	tune_low.m	Operator	BDAL@DE
Sample Name	ZHENG-XIONG-20161014-3	Instrument / Ser#	micrOTOF 10401
Comment			

Acquisition Parameter

Source Type	ESI	Ion Polarity	Positive	Set Nebulizer	0.3 Bar
Focus	Active			Set Dry Heater	180 °C
Scan Begin	50 m/z	Set Capillary	5500 V	Set Dry Gas	4.0 l/min
Scan End	2200 m/z	Set End Plate Offset	-500 V	Set Divert Valve	Waste

#	m/z	Res.	S/N	I	FWHM
1	390.2078	13476	572.2	55964	0.0290
2	391.2104	12618	37.7	18938	0.0310

Meas. m/z # Formula Score m/z err [ppm] Mean err [ppm] mSigma rdb e^- Conf N-Rule

Bruker Compass DataAnalysis 4.0 printed: 10/21/2016 8:46:34 AM Page 1 of 1

Fig. S8. HRMS spectrum of compound **3**.

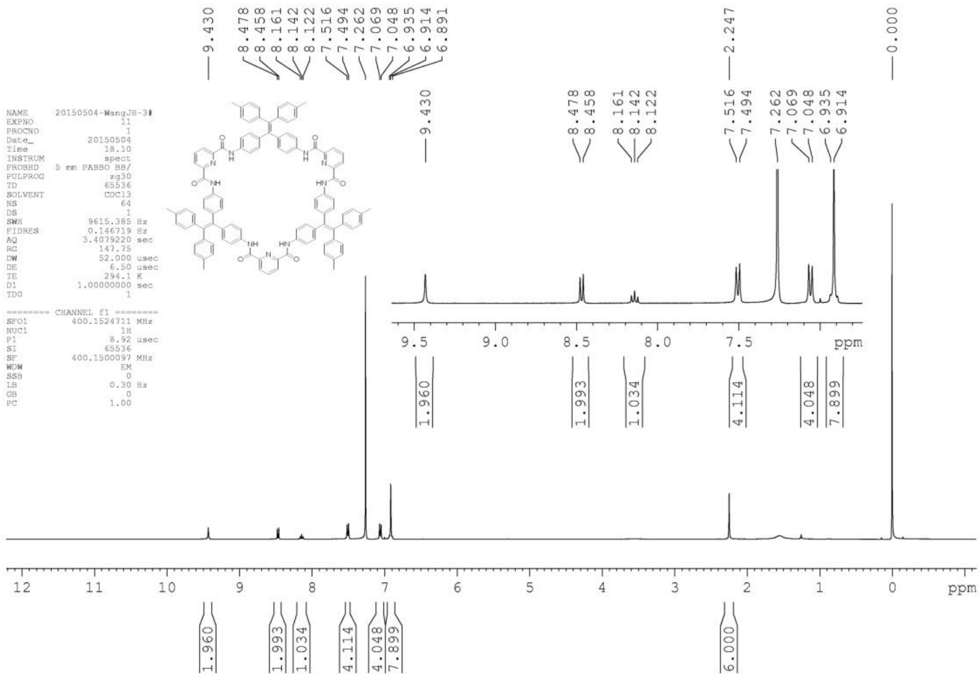

Fig. S9. ^{1}H NMR spectrum of compound **5**.

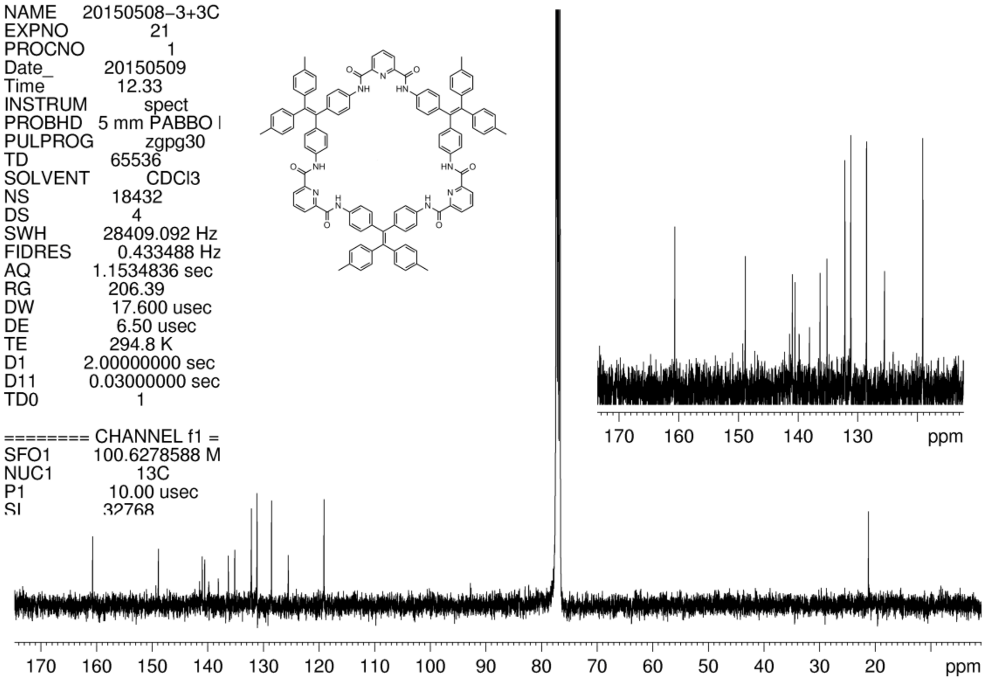

Fig. S10. ^{13}C NMR spectrum of compound **5**.

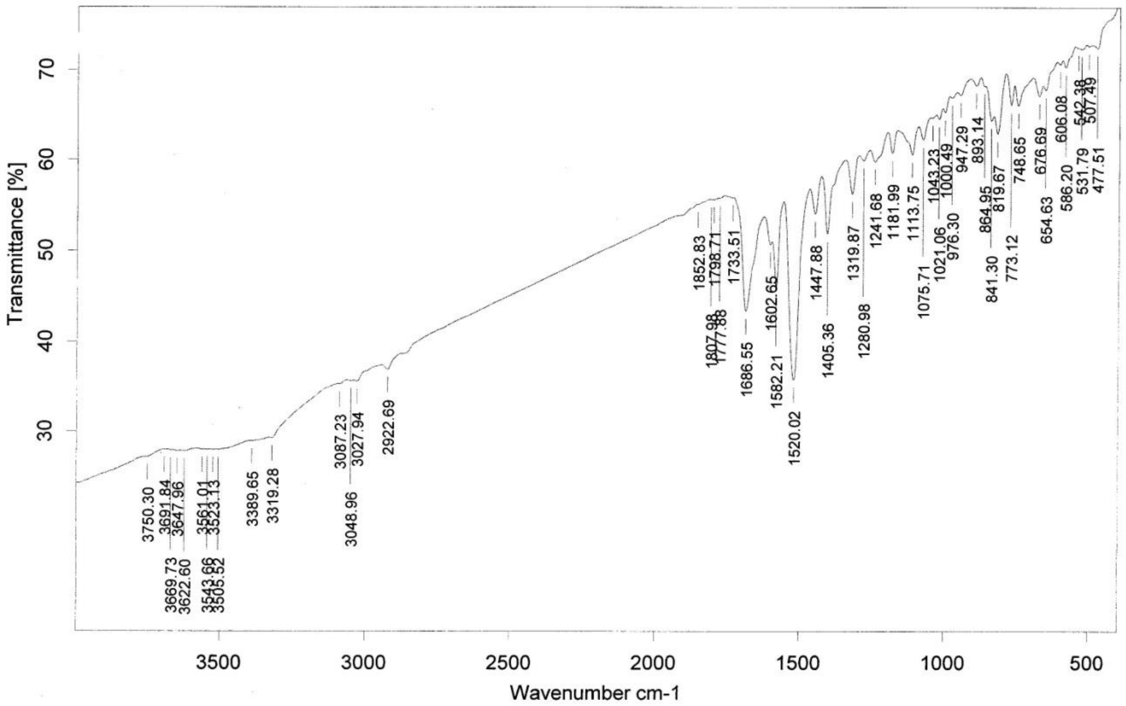

Fig. S11. IR spectrum of compound **5**.

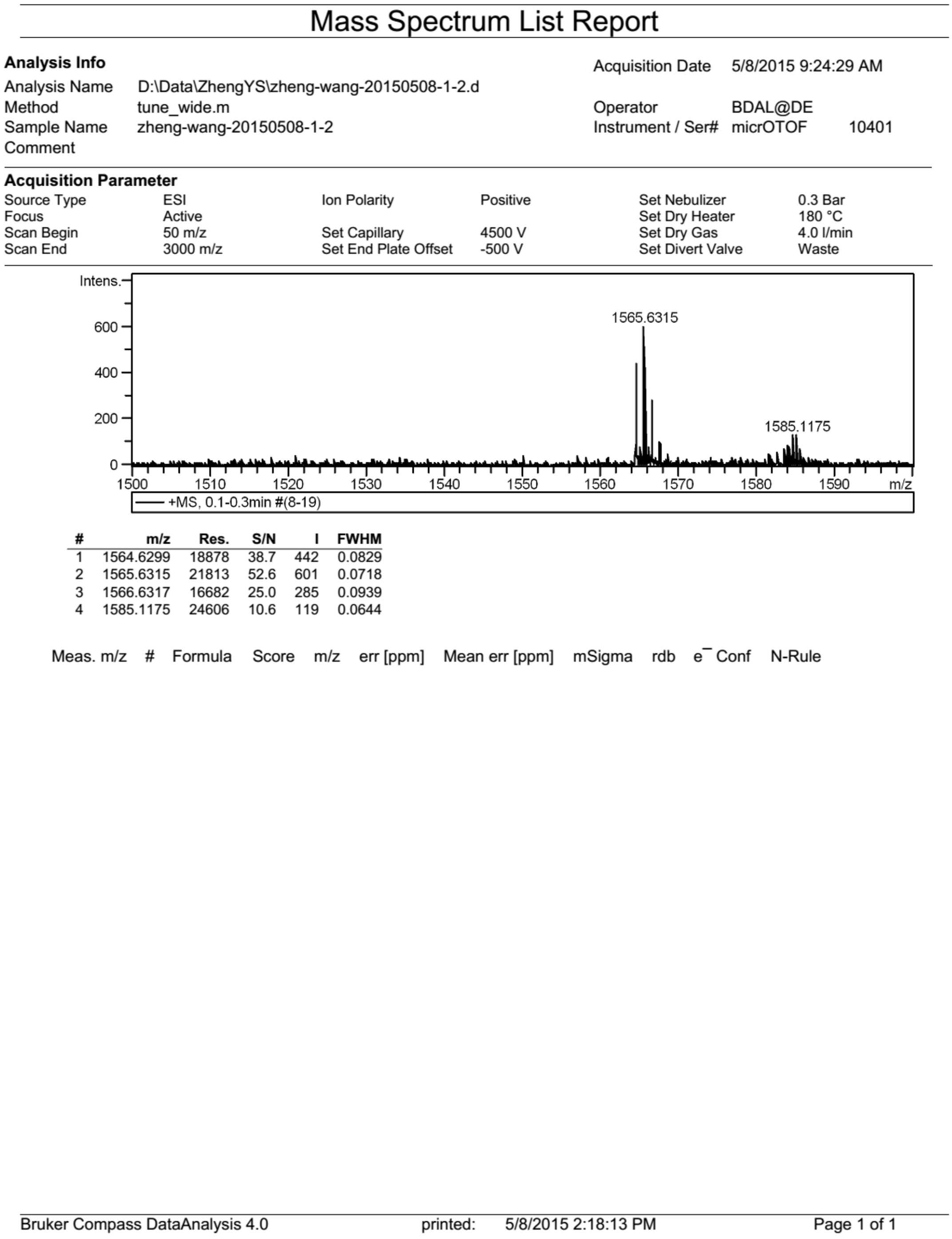

Mass Spectrum List Report

Analysis Info

Analysis Name	D:\Data\ZhengYS\zheng-wang-20150508-1-2.d	Acquisition Date	5/8/2015 9:24:29 AM
Method	tune_wide.m	Operator	BDAL@DE
Sample Name	zheng-wang-20150508-1-2	Instrument / Ser#	micrOTOF 10401
Comment			

Acquisition Parameter

Source Type	ESI	Ion Polarity	Positive	Set Nebulizer	0.3 Bar
Focus	Active			Set Dry Heater	180 °C
Scan Begin	50 m/z	Set Capillary	4500 V	Set Dry Gas	4.0 l/min
Scan End	3000 m/z	Set End Plate Offset	-500 V	Set Divert Valve	Waste

#	m/z	Res.	S/N	I	FWHM
1	1564.6299	18878	38.7	442	0.0829
2	1565.6315	21813	52.6	601	0.0718
3	1566.6317	16682	25.0	285	0.0939
4	1585.1175	24606	10.6	119	0.0644

Meas. m/z	#	Formula	Score	m/z	err [ppm]	Mean err [ppm]	mSigma	rdb	e⁻ Conf	N-Rule

Bruker Compass DataAnalysis 4.0 printed: 5/8/2015 2:18:13 PM Page 1 of 1

Fig. S12. HRMS spectrum of compound **5**.

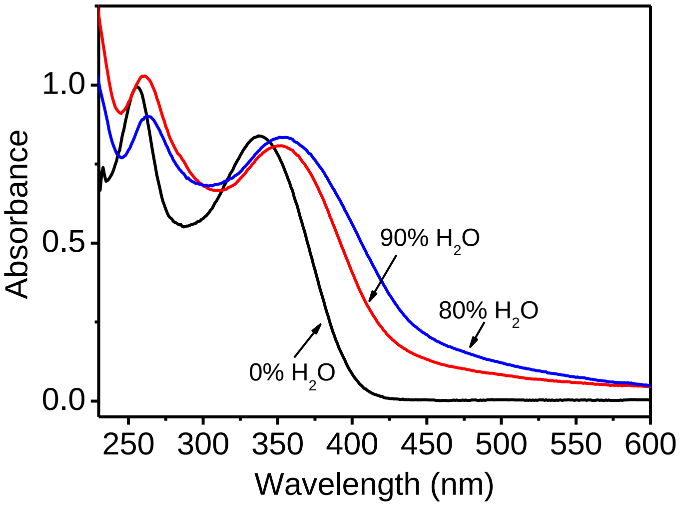

Fig. S13. The absorption spectra of **5** in H_2O/THF mixed solvent with different water fraction. [**5**] = 1.0 × 10^{-5} M. The absorption maximum wavelength λ_{max} in THF solution, 80% water and 90% water was 255/337 nm, 263/356 nm and 261/353 nm, respectively. In aggregation state, the phenyl rings of TPE unit had more conjugation with the double bond. Therefore, the absorption maximum wavelength was longer in H_2O/THF with high fraction of water than that in THF.

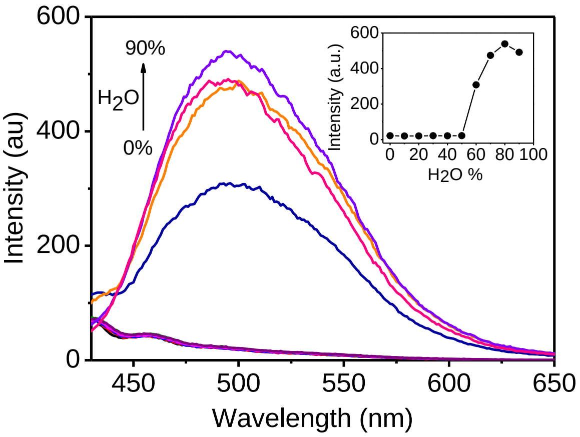

Fig. S14. Change in the fluorescence spectra of **5** in H_2O/THF mixed solvent with water fraction. Inset, curve of fluorescence intensity at 495 nm *vs* water volume percent. [**5**] = 1.0 × 10^{-5} M, λ_{ex} = 382 nm, ex/em slit widths = 3/5 nm.

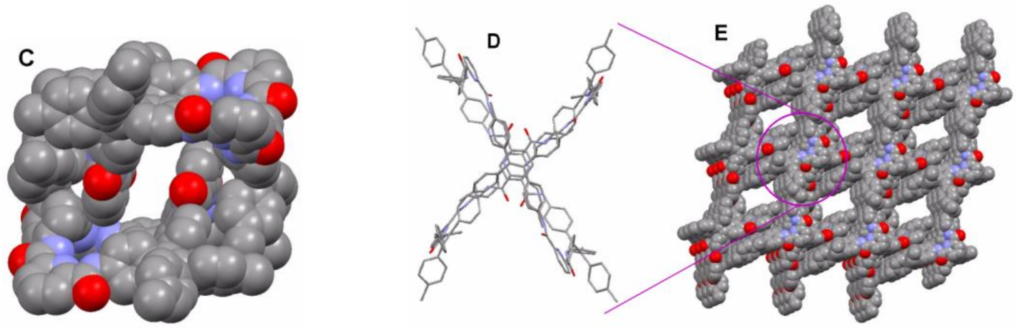

Fig. S15. (C) The cage from **5** shown in spacefill style. (D) Viewing the cage of **5** along direction perpendicular to the folded pyridyl ring. (E) The crystal channels formed by packing of the cages as nodes of the channel framework.

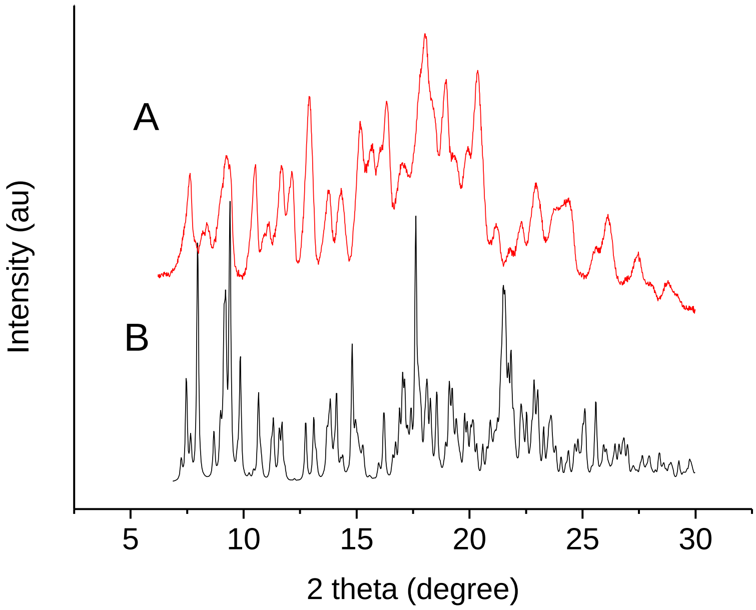

Fig. S16. (A) Powder XRD pattern of the solvent-treated crystals of **5**-TNT complex. (B) Powder XRD pattern of crystals of **5**-TNT complex simulated using Reflex module of the Mercury 3.8 software from single crystal structure.

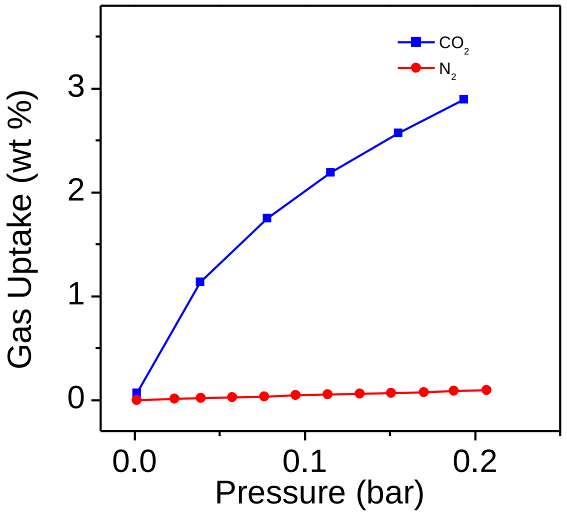

Fig. S17. Initial gas uptake slopes of **5** at 273K.

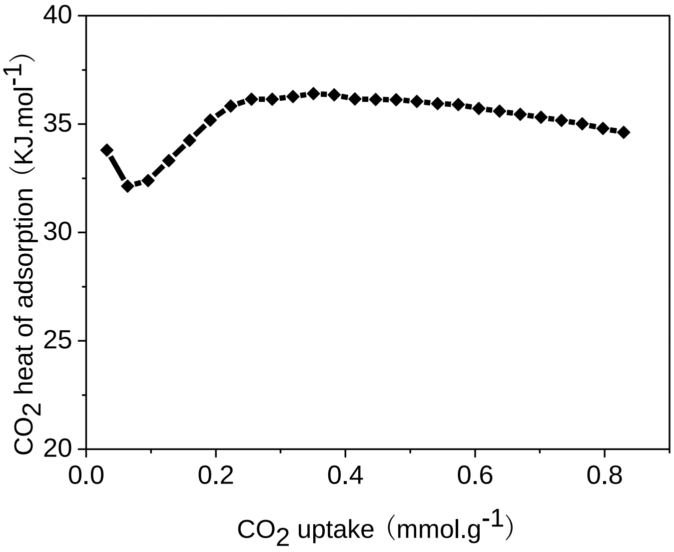

Fig. S18. Isosteric heat of adsorption for CO_2 at different CO_2 loadings.

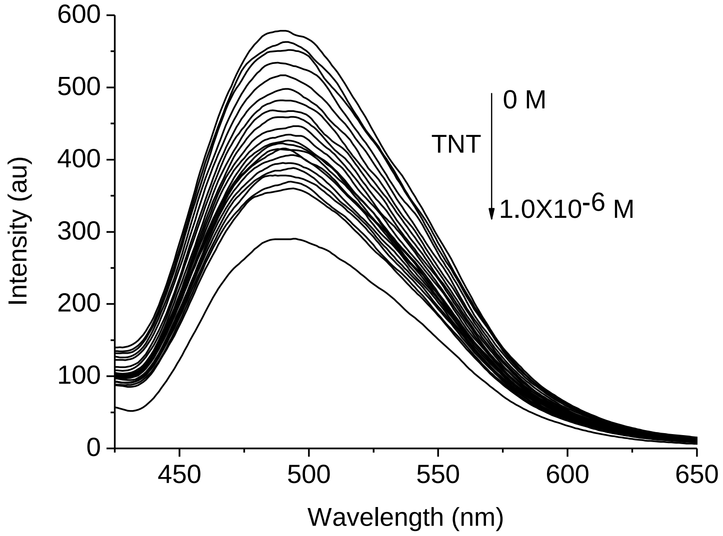

Fig. S19. Fluorescence change of **5** in 95:5 H_2O/THF with concentration of TNT. [**5**] = 1.0 × 10^{-7} M, [TNT] = (0, 0.010, 0.020, 0.050, 0.10, 0.20, 0.40, 0.60, 0.80, 1.0, 1.2, 1.4, 1.6, 1.8, 2.0, 2.5, 3.0, 3.5, 4.0, 4.5, 5.0, and 10) × 10^{-7} M. λ_{ex} = 367 nm, ex/em slit widths = 5/15 nm.

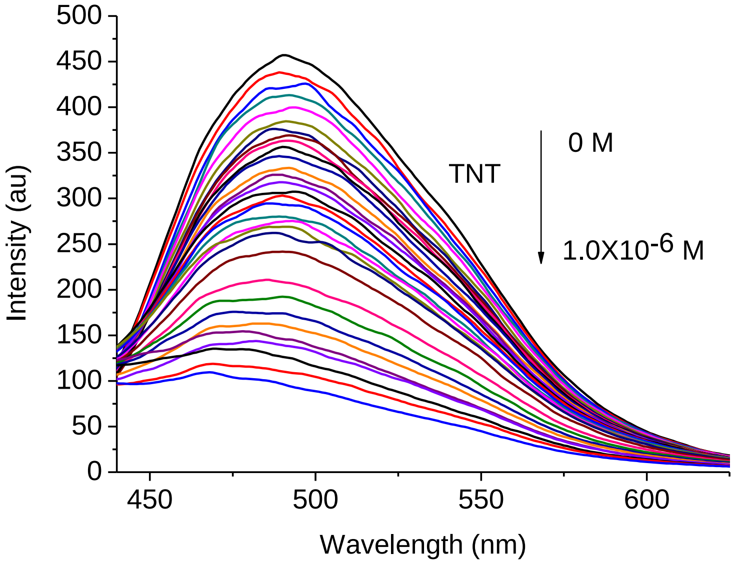

Fig. S20. Fluorescence change of **5** in 95:5 H_2O/THF in the presence of 1% $NaNO_3$ with concentration of TNT. [**5**] = 1.0 × 10^{-7} M, [TNT] = (0, 0.010, 0.020, 0.050, 0.10, 0.20, 0.40, 0.60, 0.80, 1.0, 1.2, 1.4, 1.6, 1.8, 2.0, 2.5, 3.0, 3.5, 4.0, 4.5, 5.0, 6.0, 7.0, 8.0, 9.0, 10.0, 12.0, 14.0, 16.0, 18.0, and 20) × 10^{-7} M. λ_{ex} = 367 nm, ex/em slit widths = 10/10 nm.

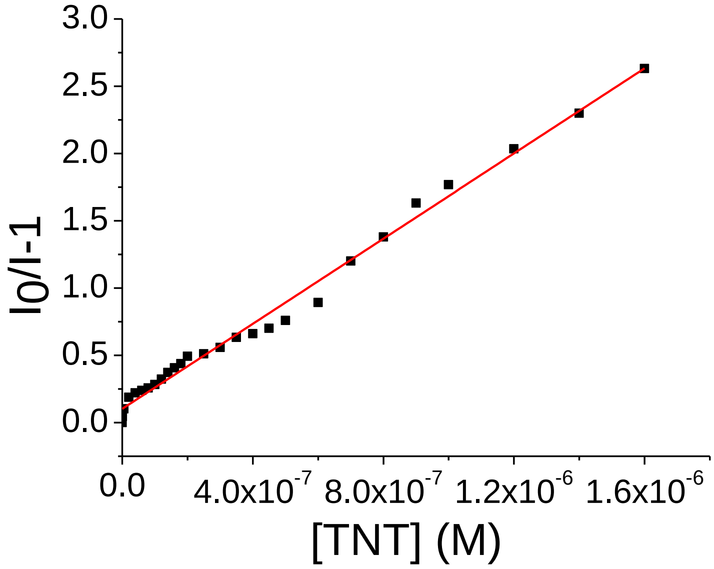

Fig. S21. The fluorescence intensity ratio ($I_0/I - 1$) of **5** with concentration of TNT. I and I_0 denote the fluorescence intensity of the suspension of **5** in the presence of 1% $NaNO_3$ with and without TNT, respectively. The red line is the fitting one. [**5**] = 1.0 × 10^{-7} M.

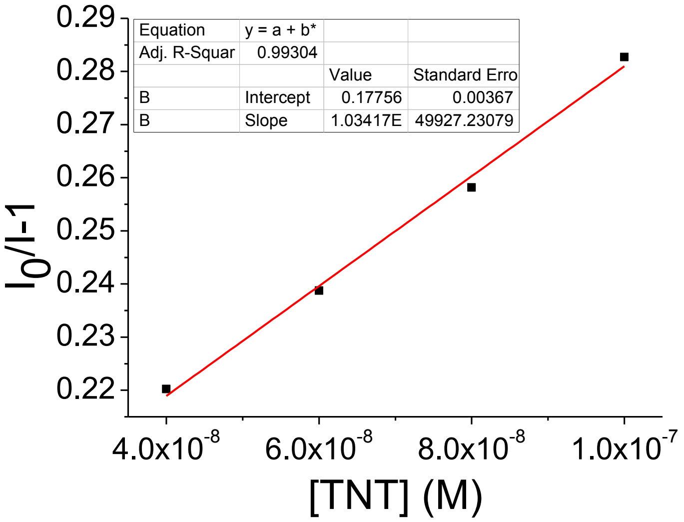

Equation	y = a + b*		
Adj. R-Squar	0.99304		
		Value	Standard Erro
B	Intercept	0.17756	0.00367
B	Slope	1.03417E	49927.23079

Fig. S22. Linear fitting for change of ($I_0/I - 1$) values of **5** with concentration of TNT in the range less than 1.0 × 10^{-7} M. The red line is the fitted one by Origin 8.0 software. I and I_0 denote the fluorescence intensity of the suspension of **5** in the presence of 1% $NaNO_3$ with and without TNT, respectively. [**5**] = 1.0 × 10^{-7} M.

In the range less than 1.0 × 10^{-7} M of added TNT, the change of ($I_0/I - 1$) values of **5** with concentration of TNT was a straight line, which had a slope of 1.03 × 10^6. At the added TNT concentration of 1.0 × 10^{-7} M, the ($I_0/I - 1$) values were measured for 5 times and gave a standard deviation of 0.0108. According detection limit = 3 × σ/k (σ, standard deviation; k, slope of the fitted straight line), the detection limit is 3 × 0.0108/(1.03 × 10^6) = 3.2 × 10^{-8} M.

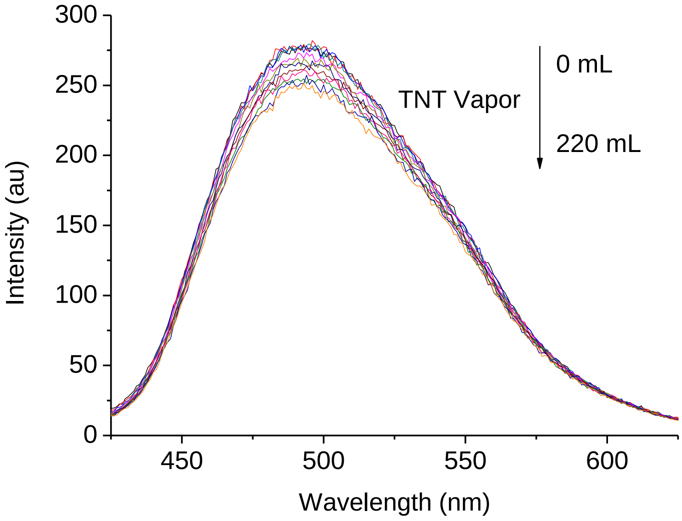

Fig. S23. Fluorescence change of **5** in 95:5 H_2O/THF in the absence of salt with volume of air containing saturated TNT vapor at 25 °C. [**5**] = 1.0 × 10^{-7} M, volume of saturated TNT vapor = 0, 20, 40, 60, 80, 100, 120, 140, 160, 180, 200, 220 mL. λ_{ex} = 366 nm, ex/em slit widths = 5/10 nm.

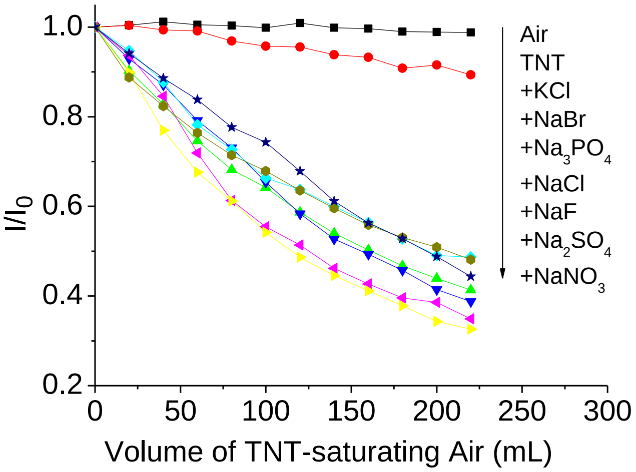

Fig. S24. Change of I/I$_0$ ratios of **5** in 95:5 H_2O/THF with volume of TNT-saturating air at 25 ^oC in the presence of 1% salts. I and I$_0$ denote the fluorescence intensity of the suspension of **5** with and without TNT vapor, respectively. [**5**] = 1.0 × 10^{-7} M.

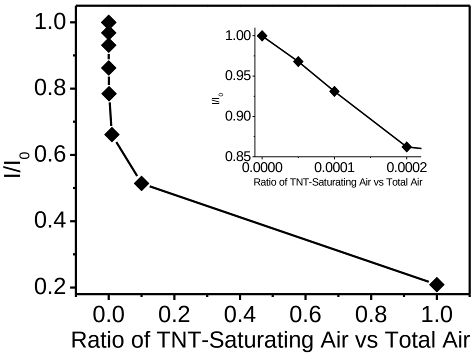

Fig. S25. Change of I/I$_0$ ratios of **5** with volume ratio of TNT-saturating air vs total air. I and I$_0$ denote the fluorescence intensity of the suspension of **5** with and without TNT vapor. [**5**] = 1.0 × 10^{-7} M.

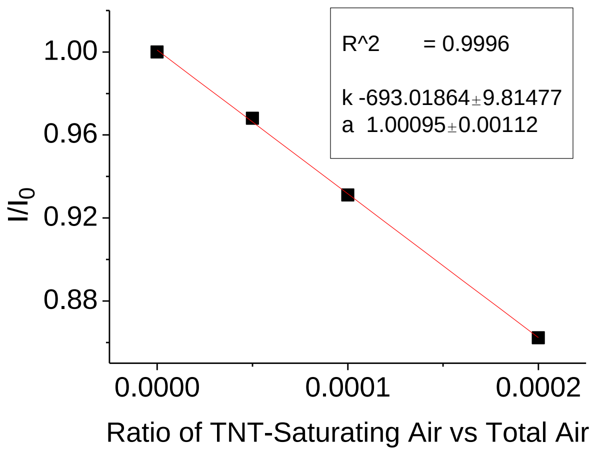

Fig. S26. Linear fitting of change of I/I_0 ratios of **5** with volume ratio of TNT-saturating air vs total air between 0 – 0.0002. I and I_0 denote the fluorescence intensity of the suspension of **5** with and without TNT vapour. [**5**] = 1.0 × 10^{-7} M.

The red line is the fitted one by Origin 7.5 software. The fitted linear equation is $y = -693.0x + 1.0010$ ($R = 0.9996$), where y is the I/I_0 ratios of **3** measured at given volume ratio of TNT-saturating air vs total air and x is the volume ratios between 0 – 0.0002. The slope of the fitted straight line is -693.0. The I/I_0 ratio of **3** at 0.000050 volume ratio of TNT-saturating air vs total air was measured for 7 times and the calculated standard deviation was 0.0057. According detection limit = 3 × σ/k (σ, standard deviation; k, slope of the fitted straight line), the detection limit is 3 × 0.0057/693 = 0.00002468, which means TNT vapor can be detected even when the volume ratio of TNT-saturating air vs total air is lowed to 0.000025. Because of the TNT-saturating air being about 7.3 ppb TN, the detection limit for TNT vapor in air should be 7.3 ppb × 0.000025 = 0.18 ppt. (see Anal. Chim. Acta, 2009, 631, 91−95, and J Fluoresc. 2010, 20, 533−540).